Hybrid numerical method for solving the harmonic Maxwell equations: III - Iterative algorithm, code and validations

J.-J. Angelini, Christian Soize, P. Soudais

HYBRID NUMERICAL METHOD FOR SOLVING THE HARMONIC MAXWELL EQUATIONS. III. ITERATIVE ALGORITHM, CODE AND VALIDATIONS

by

J. J. ANGÉLINI (*), Ch. SOIZE (*) and P. SOUDAIS (*)

ABSTRACT

In this third part of our three-part paper we first describe an iterative method for solving the linear equations of the problem. We make wide use of the mathematical properties established in Part I. Then the paper deals with the general computer code developments. This HEM 3D code is validated through applications concerning (1) a perfectly conducting dihedron with comparisons with experiment; (2) a perfectly conducting sphere experiment; and (3) dielectric spheres in homogeneous and inhomogeneous cases with and without a perfectly conducting kernel. Analytical comparisons are provided for the cases (2) and (3).

Keywords (NASA thesaurus): Electromagnetic wave — Scatter propagation — Numerical method — Finite element method — Integral equations.

(*) ONERA, BP 72, 92322 Châtillon Cedex, France.

I. – INTRODUCTION

In this third part of our three-part paper, we first present the iterative algorithm for solving the linear system of the problem, making extensive use of the properties we established in Part I.

We then discuss the aspects concerning the developments of the general HEM 3D code and its validation, which is obtained by working on examples for which there exist either an exact solution or an experimental one available. These examples validate the whole of the formulation put forth in Parts I and II.

II. – ALGORITHM FOR SOLVING THE LINEAR SYSTEM OF THE PROBLEM

II,1. – MAIN NOTATION OF LINEAR ALGEBRA

Let m be a positive integer, and the euclidian space $\mathbb{R}^m$ with respect to its canonical base is associated with the usual euclidian scalar product $\langle X, Y \rangle = \sum_{j=1}^{m} X_j Y_j$. Let $\mathbb{C}^m$ be the complexified form of $\mathbb{R}^m$ associated with the hermitian scalar product $(X, Y) = \sum_{j=1}^{m} X_j \bar{Y}_j = \langle X, \bar{Y} \rangle$ and with the norm $\| X \| = (X, X)^{1/2}$, where $\bar{Y} = (\bar{Y}_1, \ldots, \bar{Y}_m) \in \mathbb{C}^m$ is the conjugate of $Y = (Y_1, \ldots, Y_m) \in \mathbb{C}^m$..

Let $\mathbb{K} = \mathbb{R}$ or $\mathbb{C}$ and m, p be two positive integers. We will identify the vectorial space $L(\mathbb{K}^p, \mathbb{K}^m)$ of the continuous linear applications of $\mathbb{K}^p$ in $\mathbb{K}^m$ with the matrix space $\mathrm{Mat}_{\mathbb{K}}(m, p)$ of dimension $(m \times p)$, whose elements are in $\mathbb{K}$ and the space $\mathbb{K}^m$ with $\mathrm{Mat}_{\mathbb{K}}(m, 1)$. Let $Q \in \mathrm{Mat}_{\mathbb{C}}(m, p)$, and we use ^tQ to denote the transposed matrix of Q, $\bar{Q}$ the conjugate matrix, and $Q^* = {}^t\bar{Q}$ the adjoint matrix.

II,2. – STATEMENT OF THE PROBLEM

We saw in Part I that the problem is solved in two phases, to skirt the problem of the irregular frequencies.

In the first phase, we calculate a solution that may be disturbed by the irregular frequencies (solution of the system (65-1) of Part I). In the second phase, based on the solution of the linear system (63) of Part I, this disturbance is suppressed and we can therefore construct the desired solution (*see* sections VII and VIII in Part I).

The linear system (63) of Part I adapted to the linear process is associated with an invertible, symmetric, complex matrix. A hermitian matrix could be set up, but it would not have the property of

positivity. So we retain the initial structure and solve the linear system by an iterative "minimum error" method [2, 14, 16, 18]. It should be noted that the matrix of the numerical operator (63) of Part I is very hollow and similar to the unity matrix. Consequently, we have always observed a rapid convergence of the algorithm for a numerical cost that is entirely negligible compared with the other costs.

All of the numerical cost is due to the first phase. To present the algorithm we have developed for this solution, we will start by distinguishing between two cases.

II,2.1. – *First Case: Algorithm Without Lagrange Multiplier*

This is, for example, the physical situation of a perfectly conducting body, in which case, according to Part I, equation (65-1) includes no multipliers and the numerical adaptation leads to a problem of the following type.

We consider the linear system on $\mathbb{C}^m$

$$AX = S \qquad (1)$$

in which $A \in \mathrm{Mat}_{\mathbb{C}}(m, m)$, S is given in the image of A, and with the following properties. A is a noninvertible symmetric complex matrix with a kernel that is real and a real part that is definite positive in the complement of the kernel:

$$S \in \mathrm{Im}\, A \qquad (2\text{-}1)$$

$$A = {}^tA \qquad (2\text{-}2)$$

$$\ker A = \text{real vectorial subspace} \qquad (2\text{-}3)$$

$$\mathrm{R\acute{e}}\,(AX, X) > 0, \qquad \forall X \notin \ker A \qquad (2\text{-}4)$$

Under these conditions, we have:

$$\ker A \perp \mathrm{Im}\, A \qquad (3)$$

and there exists a unique solution of (1) in $\mathrm{Im}\, A$. We then solve (1) by an iterative method based on the Generalized Conjugate Residual algorithm [8, 2, 6, 14]. This algorithm is deduced immediately from the algorithm that we present hereafter, for the case with constraints, but the parts relative to the constraints are just cancelled.

Note 1: The kernel of A is due firstly to the cartesian numerical adaptation of the tangent fields on the surfaces, and also possibly to any irregular frequencies, in addition to the usual parts, *e.g.* the zero divergence functional condition, treated using constraints. As we explained in section VII,1 of Part I, the way the algorithm constructs the solution in $\mathrm{Im}\, A = (\ker A)^{\perp}$ allows us not to introduce Lagrange multipliers, so that we can require the fields to be in the tangent space.

II,2.2. — *Case 2: Algorithm With Lagrange Multipliers*

This case corresponds to the numerical adaptation of equation (65-1) of Part I, which is of the type:

$$\begin{bmatrix} A & M^* \\ M & 0 \end{bmatrix} \begin{bmatrix} X \\ \lambda \end{bmatrix} = \begin{bmatrix} S \\ 0 \end{bmatrix} \qquad (4)$$

with $A \in \mathrm{Mat}_{\mathbb{C}}(m, m)$, $M \in \mathrm{Mat}_{\mathbb{C}}(p, m)$, $X \in \mathbb{C}^m$, $\lambda \in \mathbb{C}^p$, $S \in \mathbb{C}^m$, m and p being strictly positive integers, and we look for a solution under the following hypotheses:

$$A = {}^t A \qquad (5\text{-}1)$$

ker A = real vectorial subspace

$$\ker M^* = \{0\} \qquad (5\text{-}3)$$

$$\ker A \cap \ker M = \{0\} \qquad (5\text{-}4)$$

$$\text{Ré}(AX, X) > 0, \qquad \forall X \notin \ker A \qquad (5\text{-}5)$$

We will be studying this case in detail in section III.

Note 2: (i) Hypothesis (5-3) means that the constraints are independent and implies that the matrix $MM^* \in \mathrm{Mat}_{\mathbb{C}}(p, p)$ is a definite positive hermitian. We have ker $M \neq \{0\}$, though, otherwise problem (4) would have no solution.

(ii) Hypothesis (5-4) allows us to write a consequence of the accretivity property (5-5) in the form:

$$\text{Ré}(AX, X) > 0, \quad \forall X \neq 0, \quad X \in \ker M \qquad (5\text{-}5')$$

Note 3: Assuming that we have solved the system on $\mathbb{C}^m$:

$$AX = S \qquad (6\text{-}1)$$

with the constraints:

$$MX = 0 \qquad (6\text{-}2)$$

where $A \in \mathrm{Mat}_{\mathscr{C}}(m, m)$, $M \in \mathrm{Mat}_{\mathbb{C}}(p, m)$, $S \in \mathrm{Im}\, A$, $A = {}^t A$, ker A is a real vectorial subspace, ker $M^* = \{0\}$, ker $A \oplus \ker M = \mathbb{C}^m$, then the solution of (6) is equivalent to the solution of:

$$\begin{bmatrix} A & M^* \\ M & 0 \end{bmatrix} \begin{bmatrix} X \\ \lambda \end{bmatrix} = \begin{bmatrix} S \\ 0 \end{bmatrix} \qquad (7)$$

and the unique solution is such that $\lambda = 0$.

That is, it is obvious that the unique solution of (6) is the solution of (7). Let us prove its uniqueness. Let $\{X_0, \lambda_0\}$ be the kernel of the operator (7):

$$AX_0 + M^* \lambda_0 = 0; \qquad MX_0 = 0 \qquad (8)$$

Let $Y_0 = M^* \lambda_0 = -AX_0$. We then have:

$$Y_0 \in \mathrm{Im}\, A \cap \mathrm{Im}\, M^* = (\ker A)^{\perp} \cap (\ker M)^{\perp}$$

$$\subset (\ker A \oplus \ker M)^{\perp} = (\mathbb{C}^m)^{\perp} = \{0\}.$$

Whence $\lambda_0 \in \ker M^* = \{0\}$ and

$$X_0 \in \ker A \cap \ker M = \{0\}$$

II,2.3. — *General Case for the Formulation of Part I*

The situation of section II,2.2 is a special one because of the presence of the hypothesis (5-4), which is not verified for the general case with the numerically adapted system (65-1) of Part I. But we verify that this case can be interpreted as a direct sum of cases 1 and 2 described in sections II,2.1 and II,2.2. That is, considering the operator (65-2) of Part I, we see that those tangent fields that are likely to be disturbed by the irregular frequencies are not constrained. The algorithm we will be studying in section III then constructs the solution in the space that verifies the constraints, and for the fields disturbed by the irregular frequency in the image of the operator, and this space does have an intersection reduced to $\{0\}$ with ker A.

III. — ANALYSIS OF THE ALGORITHM WITH LAGRANGE MULTIPLIERS

In this section, we describe and analyze the algorithm adapted to (4) under the hypotheses (5). We present it without conditioner, to study its properties. We then give it with the conditioner, and all of the properties remain valid.

The algorithm we have developed is derived from the Generalized Conjugate Residual algorithm. The structure of the system is used and the constraints imposed by the Lagrange multiplier are treated in a special way.

The Generalized Conjugate Residual algorithm is usually presented for real matrices with a definite positive symmetrical part. An algorithm can easily be deduced from it for a complex matrix with definite positive real part, by separating the real and imaginary parts. The algorithm is certain to converge, then, in $2m$ iterations, in which m is the dimension of the complex system. It is preferable to establish an algorithm that has the same minimization and orthogonality properties of the descent vectors, and has certain convergence in m iterations. The constants, Λ and σ, are then taken as complex. This approach therefore provides a way to accelerate the convergence, and we have in fact observed this numerically.

We have chosen to treat the Lagrange multiplier in a special way. If we treated the linear system globally without worrying about its structure, the only thing that we could say about the algorithm constructed is that it converges toward the unique solution, which verifies the constraints. Here, we require that the constraints be verified at each iteration, so that when we stop the algorithm before convergence we have an approximate solution verifying

the constraints. We will verify that all the properties of the Generalized Conjugate Residual algorithm are retained in slightly modified forms.

III,1. — ALGORITHM WITHOUT CONDITIONER

III,1.1. — Definition of the Algorithm

Let X_0 be some given element in $\mathbb{C}^m$ such that $MX_0 = 0$. This element, used for initialization, is generally taken to be zero except when we resume the iterations after a halt.

The algorithm is written as follows:

Initialization

$$X_1 = X_0, \qquad X_0 \in \ker M \qquad (9\text{-}1)$$

$$\text{solution in } \pi_0 \text{ of} : MM^* \pi_0 = M(S - AX_1) \qquad (9\text{-}2)$$

$$M^* \lambda_1 = M^* \pi_0 \qquad (9\text{-}3)$$

$$r_1 = -S + AX_1 + M^* \pi_0 \qquad (9\text{-}4)$$

$$p_1 = -r_1 \qquad (9\text{-}5)$$

$$A p_1 = -A r_1 \qquad (9\text{-}6)$$

Iterations on n

$$\text{solution in } \pi_n \text{ of} : MM^* \pi_n = MA p_n \qquad (10\text{-}1)$$

$$\Lambda_n = \frac{-(r_n, A p_n)}{\| A p_n - M^* \pi_n \|^2} \qquad (10\text{-}2)$$

$$X_{n+1} = X_n + \Lambda_n p_n \qquad (10\text{-}3)$$

$$M^* \lambda_{n+1} = M^* \lambda_n - \Lambda_n M^* \pi_n \qquad (10\text{-}4)$$

$$r_{n+1} = r_n + \Lambda_n (A p_n - M^* \pi_n) \qquad (10\text{-}5)$$

$$\text{test:} \ \| r_{n+1} \| \leq \varepsilon \| r_1 \| \ \Rightarrow \ \text{stop} \qquad (10\text{-}6)$$

$$\text{Compute } \sigma_{n+1}^i = \frac{(A r_{n+1}, A p_i - M^* \pi_i)}{\| A p_i - M^* \pi_i \|^2}$$
$$\text{for } i = 1, \ldots, n \qquad (10\text{-}7)$$

$$p_{n+1} = -r_{n+1} + \sum_{i=1}^{n} \sigma_{n+1}^i p_i \qquad (10\text{-}8)$$

$$A p_{n+1} = -A r_{n+1} + \sum_{i=1}^{n} \sigma_{n+1}^i A p_i \qquad (10\text{-}9)$$

Note 4: (i) It is noted that the algorithm requires only one product per A per iteration (and this is $A r_{n+1}$).

(ii) According to point (i) of note 2, the linear systems (9-2) and (10-1) are a unique solution. Solution (10-1) in fact allows us to write the following decomposition of $A p_n$ on the two orthogonal spaces $\text{Im} M^*$ and $\ker M$:

$$A p_n = M^* \pi_n + (A p_n - M^* \pi_n).$$

(iii) To simplify the presentation of the algorithm, we have not introduced the buffer vectors that are indispensable to the programming.

(iv) The algorithm is presented while retaining all the vectors p_n. In practice, it is possible to conserve only n' with $n' < n$.

III,1.2. — Properties of the Algorithm

We will be showing that the definition of the algorithm that uses the solutions (9-2) and (10-1) requires that the approximation X_n of rank n of the solution remain within the space in which the constraints are verified:

$$MX_n = 0, \qquad \forall n \geq 1,$$

that the iterative computation of the remainder holds to its definition:

$$r_n = AX_n + M^* \lambda_n - S,$$

that the definition (10-2) of Λ_n be capable of minimizing $\| r_{n+1} \|$ in the $A p_n - M^* \pi_n$ direction and therefore that the sequence $\{ \| r_n \| \}_n$ is decreasing monotone, that the definition (10-7) of σ_{n+1}^i requires:

$$(A p_{n+1} - M^* \pi_{n+1}, A p_i - M^* \pi_i) = 0, \qquad \forall i \leq n.$$

We will prove these properties and a few useful relations up to the rank $n+1$ by assuming $\| p_i \| \neq 0$, $\| A p_i \| \neq 0$ and $\| A p_i - M^* \pi_i \| \neq 0$ up to rank n, then we will verify that if $\| r_1 \| \neq 0$ we. have $\| p_1 \| \neq 0$, $\| A p_1 \| \neq 0$, $\| A p_1 - M^* \pi_1 \| \neq 0$, and that if $\| r_{n+1} \| \neq 0$ then $\| p_{n+1} \| \neq 0$, $\| A p_{n+1} \| \neq 0$, $\| A p_{n+1} - M^* \pi_{n+1} \| \neq 0$, which proves by recurrence that the algorithm cannot degenerate. We will finally see that this algorithm constructs a remainder of minimum norm in the space generated by the projections in $\ker M$ of the $A p_p$, that the algorithm terminates in m iterations at most.

Proposition 1: *Under hypothesis* (5-3), *$\ker M^* = \{ 0 \}$, the algorithm is such that* $\forall n \geq 1$,

$$MX_n = 0; \qquad M p_n = 0; \qquad M r_n = 0 \qquad (11)$$

Proof: — Let us show that the relations (11) are true for $n = 1$. According to the initialization (9-1), $X_1 \in \ker M$ so $MX_1 = 0$. By multiplying the two members of (9-4) to the left by M, and considering (9-2), we have $M r_1 = 0$. From (9-5) we deduce $M p_1 = 0$.

— We reason by recurrence. Let us therefore assume that we have (11) up to order n. Then, by multiplying the two members of (10-3), (10-5) and (10-8) to the left by M, and considering (10-1), we get the equalities (11) to the $n+1$ order.

Proposition 2: *The algorithm is such that* $\forall n \geq 1$:

$$r_n = AX_n + M^* \lambda_n - S \qquad (12)$$

Proof: Summing the equations (10-3) from 1 to n, we get:

$$X_n = X_1 + \sum_{j=1}^{n-1} \Lambda_j p_j \qquad (13)$$

Similarly, by summing (9-3) and (10-4) and then (9-4) and (10-5), we get:

$$M^* \lambda_n = M^* \pi_0 - \sum_{j=1}^{n-1} \Lambda_j M^* \pi_j \qquad (14)$$

$$r_n = -S + AX_1 + M^* \pi_0 + \sum_{j=1}^{n-1} \Lambda_j (A p_j - M^* \pi_j) \qquad (15)$$

By substituting (13) and (14) in (15), we get the proposition.

Proposition 3: *If* $\|A p_n - M^* \pi_n\| \neq 0$, *the definition* (10-2) *of* Λ_n *achieves the minimum of* $\|r_{n+1}\|$ *in the* $A p_n - M^* \pi_n$ *direction, and for any* $n \geq 1$ *we get:*

$$\|r_{n+1}\| \leq \|r_n\| \qquad (16\text{-}1)$$

$$(r_{n+1}, A p_n) = 0 \qquad (16\text{-}2)$$

Proof: — We write the norm of the remainder using (10-5):

$$\|r_{n+1}\|^2 = \|r_n\|^2 + \bar\Lambda_n (r_n, A p_n - M^* \pi_n)$$
$$+ \Lambda_n (A p_n - M^* \pi_n, r_n) + \Lambda_n \bar\Lambda_n \|A p_n - M^* \pi_n\|^2$$

$$= \|r_n\|^2 + a_n \left(\Lambda_n + \frac{b_n}{a_n} \right) \left(\bar\Lambda_n + \frac{\bar b_n}{a_n} \right) - \frac{b_n \bar b_n}{a_n}$$

$$= \|r_n\|^2 + a_n \left(\Lambda_n + \frac{b_n}{a_n} \right) \overline{\left(\Lambda_n + \frac{b_n}{a_n} \right)} - \frac{b_n \bar b_n}{a_n}$$

with:

$$a_n = \|A p_n - M^* \pi_n\|^2$$
$$b_n = (r_n, A p_n - M^* \pi_n)$$

This last expression shows that the minimum of $\|r_{n+1}\|^2$ is obtained for

$$\Lambda_n = -\frac{b_n}{a_n} = -\frac{(r_n, A p_n - M^* \pi_n)}{\|A p_n - M^* \pi_n\|^2}$$
$$= \frac{-(r_n, A p_n) + (M r_n, \pi_n)}{\|A p_n - M^* \pi_n\|^2},$$

which does correspond to the definition (10-2), considering Proposition 1.
— We then have:

$$\|r_{n+1}\|^2 = \|r_n\|^2 - \frac{|(r_n, A p_n)|^2}{\|A p_n - M^* \pi_n\|^2}$$
$$\|r_{n+1}\|^2 \leq \|r_n\|^2 \qquad (17)$$

— We multiply (10-5) to the right by $A p_n$:

$$(r_{n+1}, A p_n) = (r_n, A p_n) + \Lambda_n (A p_n - M^* \pi_n, A p_n).$$

Considering the solution (10-1) we deduce from this that:

$$(r_{n+1}, A p_n) = (r_n, A p_n)$$
$$+ \Lambda_n (A p_n - M^* \pi_n, A p_n - M^* \pi_n).$$

The definition (10-2) of Λ_n then proves (16-2).

Proposition 4: *If* $\|A p_i - M^* \pi_i\| \neq 0$, $1 \leq i \leq n$, *the definition* (10-7) *of the* σ_{n+1}^i *shows that:*

$$\left. \begin{array}{l} (A p_i, A p_{n+1} - M^* \pi_{n+1}) = 0 \\ \quad \text{for} \quad i < n+1 \end{array} \right\} \qquad (18\text{-}1)$$

$$\left. \begin{array}{l} (A p_i - M^* \pi_i, A p_{n+1} - M^* \pi_{n+1}) = 0 \\ \quad \text{for} \quad i < n+1 \end{array} \right\} \qquad (18\text{-}2)$$

$$(A p_{n+1}, A p_i - M^* \pi_i) = 0 \qquad \text{for} \quad i < n+1 \qquad (18\text{-}3)$$

and the property (16-2) *is extended as follows:*

$$(A p_i, r_{n+1}) = 0 \qquad \forall i < n+1 \qquad (19)$$

Moreover:

$$(A p_{n+1}, r_{n+1}) = -(A r_{n+1}, r_{n+1}) \qquad (20)$$

Proof: Considering the solution (10-1), the equations (18-1), (18-2) and (18-3) are equivalent and so we just have to prove (18-3).
We write (10-9) at order 1, multiplied to the right by $A p_1 - M^* \pi_1$:

$$(A p_2, A p_1 - M^* \pi_1)$$
$$= -(A r_2, A p_1 - M^* \pi_1) + \sigma_2^1 (A p_1, A p_1 - M^* \pi_1)$$

The definition of σ_2^1 does prove the property (18-3) at the first order.
We assume the property to be true up to the order n, and in the same way we multiply (10-9) to the right by $A p_j - M^* \pi_j$ for $j < n+1$:

$$(A p_{n+1}, A p_j - M^* \pi_j) = -(A r_{n+1}, A p_j - M^* \pi_j)$$
$$+ \sum_{i=1}^{n} \sigma_{n+1}^i (A p_i, A p_j - M^* \pi_j)$$

According to the recurrence hypothesis, all of the terms in the sum are zero except $(A p_j, A p_j - M^* \pi_j)$. The definition σ_{n+1}^j then proves:

$$(A p_{n+1}, A p_j - M^* \pi_j) = 0$$

— To prove (19), we again proceed by recurrence. The property for $n = 1$ is the property (16-2). We assume it to be true up to order n, and then we multiply (10-5) to the left by $A p_i (i < n)$:

$$(A p_i, r_{n+1}) = (A p_i, r_n) + \bar\Lambda_n (A p_i, A p_n - M^* \pi_n)$$

The property (18-1), combined with the recurrence hypothesis, shows that:

$$(A p_i, r_{n+1}) = 0, \qquad i < n$$

and we have (16-2) $(A p_n, r_{n+1}) = 0$ for $i = n$.

– The property (20) is deduced from (10-9) multiplied to the right by r_{n+1}:

$$(A p_{n+1}, r_{n+1})$$

$$= -(A r_{n+1}, r_{n+1}) + \sum_{i=1}^{n} \sigma_{n+1}^{i} (A p_i, r_{n+1})$$

Considering (19), we do get (20).

Proposition 5: *Having presented the algorithm* (9)-(10), *under the hypotheses of the problem — accredivity* (5-5) $\text{Re}(AX, X) > 0$, $\forall X \notin \ker A$ *and the property* (5-4) – $\ker A \cap \ker M = \{0\}$, *it cannot degenerate.*

– *If* $r_{n+1} \neq 0$ *then*

$$p_{n+1} \neq 0, \qquad A p_{n+1} \neq 0, \qquad A p_{n+1} - M^* \pi_{n+1} \neq 0,$$

and it is still possible to compute Λ_{n+1} *and* σ_{n+2}^{i}.

– *If* $r_{n+1} = 0$, *then the algorithm stops on the exact solution.*

In all of the following, we consider only the case $\|r_i\| \neq 0$ for $i = 1, \ldots, (n+1)$.

Proof: This result is established by recurrence. At order 1, we have $i = 1, \ldots, (n+1)$. Since $r_1 \neq 0$, then $p_1 \neq 0$ and $p_1 \in \ker M$ (Proposition 1) considering (5-4) $A p_1 \neq 0$. Let us assume that $A p_1 - M^* \pi_1 = 0$. Then

$$\text{Re}(A p_1, p_1) = \text{Re}(M^* \pi_1, p_1) = \text{Re}(\pi_1, M p_1) = 0$$

since $p_1 \in \ker M$. But this is in contradiction with the property (5-5'):

$$\forall X \in \ker M, \qquad X \neq 0, \qquad \text{Re}(AX, X) \neq 0.$$

Since $\|r_i\| \neq 0$ up to order n (or else the algorithm would have stopped on the exact solution, $\|p_i\| \neq 0$, $\|A p_i\| \neq 0$, and $\|A p_i - M^* \pi_i\| \neq 0$, properties (16) to (20) that have been shown, hold up to the rank $n+1$ (they do not make use of $\|p_{n+1}\| \neq 0$, $\|A p_{n+1}\| \neq 0$, $\|A p_{n+1} - M^* \pi_{n+1}\| \neq 0$. As $\|r_{n+1}\| \neq 0$, then Proposition 1 combined with (5-5') proves that $\text{Ré}(A r_{n+1}, r_{n+1}) > 0$ and therefore, according to (20):

$$\text{Re}(A p_{n+1}, r_{n+1}) \neq 0 \qquad (21)$$

We conclude from this that $\|p_{n+1}\| \neq 0$ and $\|A p_{n+1}\| \neq 0$. Assuming $\|A p_{n+1} - M^* \pi_{n+1}\| = 0$, we replace $A p_{n+1}$ by $M^* \pi_{n+1}$ to use Proposition 1:

$$\text{Re}(A p_{n+1}, r_{n+1})$$
$$= \text{Re}(M^* \pi_{n+1}, r_{n+1}) = \text{Re}(\pi_{n+1}, M r_{n+1}) = 0.$$

which is incompatible with (21).

Proposition 6: *The vector families* $\{A p_n - M^* \pi_n\}_n$, $\{A p_n\}_n$, $\{p_n\}_n$ *and* $\{r_n\}_n$ *are each free and we have:*

$$(r_{n+1}, A r_j) = 0 \qquad \text{for} \quad j < n+1 \qquad (22)$$

Proof: Since $\|r_i\| \neq 0$, $\forall i \in \{1, \ldots, n\}$, by Proposition 5 we then have $\|A p_i - M^* \pi_i\| \neq 0$, $\forall i \in \{1, \ldots, n\}$. The property (18-2),

$$(A p_i - M^* \pi_i, A p_j - M^* \pi_j) = 0 \quad (1 \leq j \leq n \text{ and } i \neq j),$$

then shows that the family $\{A p_n - M^* \pi_n\}_n$ is free and orthogonal. We then draw from this the property for the family $\{A p_n\}_n$ and then for $\{p_n\}_n$.

We then show by recurrence that the $\{p_n\}_n$ and $\{r_n\}_n$ families generate the same space. That is, the property is evident at order 1, considering the initialization (9-5). So we assume it is true up to order n. The recurrence hypothesis and (10-8) show that the space generated by vectors $\{p_i\}$, $i \in \{1, \ldots, n+1\}$ is included in the space generated by $\{r_i\}$ $i \in \{1, \ldots, n+1\}$. The family $\{r_n\}_n$ is therefore free and the two spaces are identical.

To show (22), we multiply (10-9) to the left by r_{n+1}:

$$(r_{n+1}, A p_j) = -(r_{n+1}, A r_j) + \sum_{i=1}^{j} \overline{\sigma_{j+1}^{i}} (r_{n+1}, A p_i)$$

Considering (19), this does give us (22).

Proposition 7: *The algorithm constructs the best approximation of the solution in the .affine space* $X_0 + \{A p_1 - M^* \pi_1, \ldots, A p_n - M^* \pi_n\}$, *that is, where* $\|r_{n+1}\|$ *is minimum. Proposition 6 then proves that the algorithm terminates in m iterations at most.*

Proof: We first show the following property:

$$\left. (r_j, A p_{n+1} - M^* \pi_{n+1}) = (r_1, A p_{n+1} - M^* \pi_{n+1}) \atop j \leq n+1 \right\} \quad (23)$$

To do so, we multiply (10-5) written for $j < n+1$ to the right by $A p_{n+1} - M^* \pi_{n+1}$:

$$(r_{j+1}, A p_{n+1} - M^* \pi_{n+1}) = (r_j, A p_{n+1} - M^* \pi_{n+1})$$
$$+ \Lambda_j (A p_j - M^* \pi_j, A p_{n+1} - M^* \pi_{n+1})$$

Considering (18-2), we get:

$$(r_{j+1}, A p_{n+1} - M^* \pi_{n+1})$$
$$= (r_j, A p_{n+1} - M^* \pi_{n+1}), \qquad \forall j < n+1$$

and in particular

$$\text{Re}(r_j, A p_{n+1} - M^* \pi_{n+1})$$
$$= \text{Re}(r_1, A p_{n+1} - M^* \pi_{n+1}), \qquad \forall j \leq n+1$$

We write $\|r_{n+1}\|^2$ using (15) and the initialization (9-4) while using (18-2) to analyze the $(A\,p_i - M^* \pi_i, A\,p_j - M^* \pi_j)$ terms for $i \neq j$:

$$\|r_{n+1}\|^2 = \|r_1\|^2 + \sum_{i=1}^{n} \Lambda_i (A\,p_i - M^* \pi_i, r_1)$$

$$+ \sum_{i=1}^{n} \bar{\Lambda}_i (r_1, A\,p_i - M^* \pi_i)$$

$$+ \sum_{i=1}^{n} \Lambda_i^2 \|A\,p_i - M^* \pi_i\|^2$$

The Λ_i' necessary for $\|r_{n+1}\|$ to be minimum on the orthogonal vectors $A\,p_i - M^* \pi_i$ are found by following the same line of reasoning as in the proof of Proposition 3:

$$\Lambda_i' = \frac{-(r_1, A\,p_i - M^* \pi_i)}{\|A\,p_i - M^* \pi_i\|^2}$$

We then use (23) and then the Proposition 1 $(M\,r_n = 0)$:

$$\Lambda_i' = \frac{-(r_i, A\,p_i - M^* \pi_i)}{\|A\,p_i - M^* \pi_i\|^2} = \frac{-(r_i, A\,p_i)}{\|A\,p_i - M^* \pi_i\|^2}$$

Proposition 8: *Let* φ_n *be such that:*

$$\varphi_n = \frac{|(A\,r_n, r_n)|^2}{\|r_n\|^2 \|A\,p_n - M^* \pi_n\|^2} = \frac{I_n J_n}{K_n} \quad (24\text{-}1)$$

$$I_n = \frac{|(A\,r_n, r_n)|}{\|r_n\|^2}; \qquad J_n = \frac{|(A\,p_n, p_n)|}{\|p_n\|^2};$$
$$K_n = \frac{\|A\,p_n - M^* \pi_n\|^2}{\|p_n\|^2} \quad (24\text{-}2)$$

Then there exists a real φ_0 *such that:*

$$\forall n \geq 1, \quad 0 < \varphi_0 \leq \varphi_n \leq 1 \quad (25\text{-}1)$$

$$\|r_{n+1}\| = \|r_n\| \sqrt{1 - \varphi_n} \quad (25\text{-}2)$$

Proof: The equality (25-2), with φ_n given by (24) is found from (17) with (20). For the middle part of this same equation (24-1), we again use (20) which, considering Proposition 1, can be written:

$$(A\,r_n, r_n) = -(A\,p_n, r_n) = -(A\,p_n - M^* \pi_n, r_n)$$

We then get (24) by replacing r_n with (10-8), using the orthogonality relation (17-1) and Proposition 1.

According to Proposition 1, hypothesis (5-5), and since $\|r_n\| \neq 0$, we see that $\forall n \geq 1$, I_n is strictly positive. $\underset{X \in \ker M, \; \|X\|=1}{\text{Inf}} |(AX, X)|$ is a lower bound of it, the set $\{ X \in \ker M, \|X\| = 1 \}$ is closed and of empty intersection with $\ker A$ (hypothesis (5-4)), so Inf

denoted a_0 is attained and is nonzero:

$$\underset{p_n, \, n \in \mathbb{N}}{\text{Inf}} \; I_n \leq a_0 \quad \text{with} \quad a_0 > 0 \quad (26\text{-}1)$$

We remember that if we have $\ker M = \operatorname{Im} A$, a_0 is the norm of the smallest nonzero eigenvalue of A.

The vector p_n satisfies the same conditions as r_n and the lower bound found for I_n is also a lower bound for J_n:

$$\underset{p_n, \, n \in \mathbb{N}}{\text{Inf}} \; J_n \leq a_0 \quad \text{with} \quad a_0 > 0 \quad (26\text{-}2)$$

Finally, we can verify that

$$\|A\,p_n - M^* \pi_n\|^2 = \|A\,p_n\|^2 - \|M^* \pi_n\|^2$$

which yields:

$$K_n \leq \frac{\|A\,p_n\|^2}{\|p_n\|^2}$$

and therefore

$$\underset{p_n, \, n \in \mathbb{N}}{\text{Sup}} \; K_n \leq \underset{X \in \ker M, \; \|X\|=1}{\text{Sup}} \|AX\|^2 = b_0$$
$$\text{with} \quad b_0 > 0. \quad (26\text{-}3)$$

The three inequalities (26) then lead to (25-1).

III,2. – ALGORITHM WITH CONDITIONER

III,2.1. – *Definition of the Conditioner*

To condition problem (4), we introduce the hermitian, definite positive conditioning matrix $D \in \operatorname{Mat}_{\mathbb{C}}(m, m)$:

$$D^* = D; \quad (DX, X) > 0, \quad \forall X \in \mathbb{C}^m, \quad \|X\| \neq 0 \quad (27)$$

Consequently, there exists an invertible $L \in \operatorname{Mat}_{\mathbb{C}}(m, m)$ such that:

$$D = LL^* \quad (28)$$

III,2.2. – *Construction of the Algorithm With Conditioner*

Take $\hat{X}$ and $\hat{S}$ in $\mathbb{C}^m$ such that:

$$X = L\hat{X}; \qquad \hat{S} = L^* S \quad (29)$$

Problem (4) is then written:

$$\begin{bmatrix} \hat{A} & \hat{M}^* \\ \hat{M} & 0 \end{bmatrix} \begin{bmatrix} \hat{X} \\ \lambda \end{bmatrix} = \begin{bmatrix} \hat{S} \\ 0 \end{bmatrix} \quad (30\text{-}1)$$

$$\hat{A} = L^* A L; \qquad \hat{M} = M L \quad (30\text{-}2)$$

It will be noted that problem (30) does not derive directly from hypotheses (5), *e. g.* $\hat{A} \neq {}^t\hat{A}$. However, following the line of reasoning developed in section III,1, we verify that all of the properties of the algorithm previously established still hold. For example, we still have ker $\hat{A} \perp \text{Im}\,\hat{A}$.

Using variable change (29), we arrive at the algorithm with conditioner.

III,2.3. — *Algorithm With Conditioner*

The algorithm that follows is given in a form that minimizes the number of operations. This avoids having to show the products by L, L^* or L^{-1}.

Let X_0 be some given element in $\mathbb{C}^m$ such that $MX_0 = 0$. This element, used at initialization, is generally taken to be zero except at times when the iterations are resumed after a halt.

We introduce the operator $\text{Proj} : \mathbb{C}^m \to \mathbb{C}^m$ such that

$$\forall\, T \in \mathbb{C}^m \text{ we have } b = \text{Proj}\,(T)$$

with:

$$(MDM^*)\,\pi = MDT \tag{31-1}$$

$$b = M^*\,\pi \tag{31-2}$$

The algorithm is written as follows:
Initialization

$$X_1 = X_0, \qquad X_0 \in \ker M \tag{32-1}$$

$$T_1 = S - AX_1 \tag{32-2}$$

$$b_1 = \text{Proj}\,(T_1) \tag{32-3}$$

$$Y_1 = b_1 \tag{32-4}$$

$$\rho_1 = -T_1 + b_1 \tag{32-5}$$

$$r_1 = D\rho_1 \tag{32-6}$$

$$\|\rho_1\|_D^2 = (D\rho_1,\ \rho_1) = (r_1,\ \rho_1) \tag{32-7}$$

$$p_1 = -r_1 \tag{32-8}$$

$$u_1 = A\,r_1 \tag{32-9}$$

$$q_1 = A\,p_1 = -u_1 \tag{32-10}$$

$$\alpha_1 = -(r_1,\ q_1) \tag{32-11}$$

Iterations on n

$$b_n = \text{Proj}\,(q_n) \tag{33-1}$$

$$c_n = q_n - b_n \tag{33-2}$$

$$T_n = Dc_n \tag{33-3}$$

$$\|c_n\|_D^2 = (Dc_n,\ c_n) = (T_n,\ c_n) \tag{33-4}$$

$$\Lambda_n = \frac{\alpha_n}{\|c_n\|_D^2} \tag{33-5}$$

$$X_{n+1} = X_n + \Lambda_n p_n \tag{33-6}$$

$$Y_{n+1} = Y_n - \Lambda_n b_n \tag{33-7}$$

$$\rho_{n+1} = \rho_n + \Lambda_n c_n \tag{33-8}$$

$$r_{n+1} = D\rho_{n+1} \tag{33-9}$$

$$\|\rho_{n+1}\|_D^2 = (D\rho_{n+1},\ \rho_{n+1}) = (r_{n+1},\ \rho_{n+1}) \tag{33-10}$$

test : $\|\rho_{n+1}\|_D \le \varepsilon \|\rho_1\|_D \quad \Rightarrow \quad$ stop $\tag{33-11}$

$$u_{n+1} = A\,r_{n+1} \tag{33-12}$$

Compute $\sigma_{n+1}^i = \dfrac{(u_{n+1},\ Dc_i)}{(Dc_i,\ c_i)} \tag{33-13}$

$$\text{for } i = 1,\ \dots,\ n$$

$$p_{n+1} = -r_{n+1} + \sum_{i=1}^{n} \sigma_{n+1}^i\,p_i \tag{33-14}$$

$$q_{n+1} = -u_{n+1} + \sum_{i=1}^{n} \sigma_{n+1}^i\,q_i \tag{33-15}$$

$$\alpha_{n+1} = -(r_{n+1},\ q_{n+1}) \tag{33-16}$$

Note 5: (i) The algorithm is presented with all of the vectors p_i, q_i, c_i, but it is possible to retain only n' with $n' < n$, in practice.

(ii) We have introduced buffer vectors (T_n, b_n, r_n, u_n) which are practical for the computer process but are of no mathematical relevance.

(iii) It will be noted that the vector Y_{n+1} contains the rank $n+1$ approximation from the $M^*\lambda$ part of the solution.

(iv) It will also be noted that the construction of each b_n given by (33-1) requires that the linear system (31-1) be solved, which is done by the conjugate gradient method preconditioned by the diagonal.

(v) It is possible to drop the sequence of vectors c_i, but this means computing $\text{Proj}\,(u_n)$ and therefore having to solve an additional linear system.

IV. — HEM 3D SOFTWARE

A general code called HEM 3D (standing for "multidomain Maxwell harmonic electromagnetism") has been developed on the basis of the theory explained throughout this three-part paper. It can currently simulate the general case of multiconductor, multidielectric volume bodies.

IV,1. — GENERAL ASPECTS

The computer structure was developed in the following context.

1. The code is written in FORTRAN 77 standard to make it easier to implant on any 64-bit machine.

2. It is written with optimum vectorization possibilities in mind for CRAY-type vectorial processors. The loops in the program were also colored, to deal with the assembly of the local operators.

3. The code can handle very large 3-D problems with no I/O s during the solution. Dynamic memory management was incorporated.

4. The code architecture was organized to allow rapid installation on parallel-processor computers.

IV,2. – DATA STRUCTURE

Each dielectric volume domain Ω_n with its boundary $\partial\Omega_n$ is meshed on its own. So the data structure for a given problem is defined by:
– the volume grid data of each dielectric body Ω_n with the material characteristics;
– the surface grid for each boundary $\partial\Omega_n$;
– the surface grid for the boundary of each conductive body.

The formulation requires the elements to be grouped:
– volume group: four-node tetrahedrons;
– outer conductive surface group (Γ_c): three-node triangles;
– outer dielectric surface group (Γ_d): three-node triangles;
– dielectric-conductor interface group (Γ_{cd}): three-node triangles;
– dielectric-dielectric interface group ($\Gamma_{nn'}$): superposition of three 3-node triangles.

The code automatically groups these elements (and subgroups them according to their material characteristics, i. e. homogeneous, inhomogeneous, isotropic, anisotropic, lossy and nonlossy). The code also automatically orients all of the surfaces.

V. – APPLICATIONS AND VALIDATION

This section presents a number of applications that allow us to validate the different points of the formulation. We find:

– The case of the perfect conductor. The results are compared with analytical results for the sphere, which validates the treatment of the irregular frequencies for a volume object, then with the case of the cone-sphere for which there is a point effect, and finally the case of the dihedron compared with experimental results, which validates the treatment of slender objects.

– A nonlossy dielectric. The case of the sphere is compared with analytical results, validating the dielectric volume part and the magnetic induction zero divergence constraint.

– The hybrid case of a dielectric with a perfect conductor. A sphere with metal core is compared with analytical results, to validate the treatment of the dielectric perfect conductor interfaces.

– The hybrid case of two lossy dielectrics. Two concentric spherical layers are compared with analytical results to validate the treatment of dielectric-dielectric interfaces.

All of the analytical solutions we have used for the spheres were obtained by Mie's series expansion, presented in [21].

V,1. – PERFECT CONDUCTOR

V,1.1. – *Metal Sphere*

The object considered is a sphere of radius $a = 1$ m made of a perfect conductor. We analyze the equivalent cross section (RCS) for a bandwidth of [0.8, 5.0] meters. The grid of the surface Γ_c presented in figure 1 has 578 nodes and 1,152 elements.
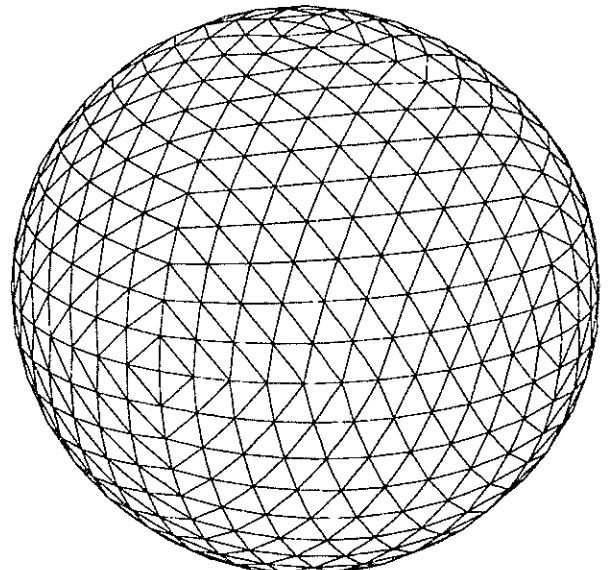

Fig. 1. – Grid for the metal sphere.

The data computed for this configuration is compared with analytical data in figure 2, the ordinate being
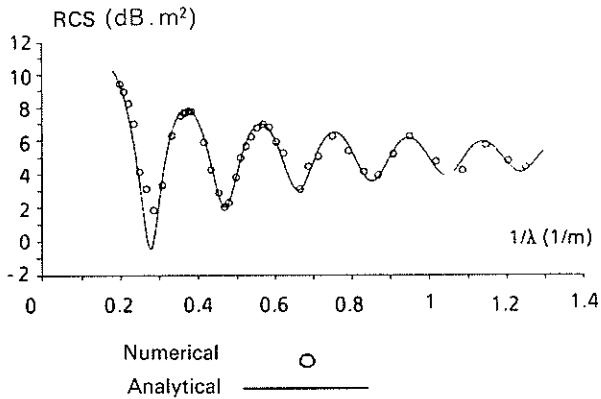
RCS (dB.m²)

Numerical   O

Analytical   ―――――

Fig. 2. — Computation of RCS on a metal sphere.

$$10 \log_{10} \lim_{R \to \infty} 4\pi R^2 \frac{\| E_r \|^2}{\| E_i \|^2},$$ where E_r is the scattered field at a distance R from the object and E_i is the incident field.

The irregular frequencies within the band being analyzed are known exactly in this case [26, 10], and correspond to wavelengths 0.82 m, 1.08 m, 1.40 m and 2.28 m.

The good agreement can be seen between predictions by the formulation developed and the analytical results, and chiefly that the irregular frequencies do not disturb the solution.

V,1.2. — Metal Cone-Sphere

The object here is a cone with an apex semi-angle of 12.5°, tangent to a sphere of radius $a = 1$ m, made of a perfect conductor. The RCS is studied for the wavelength $\lambda = 0.974$ m, the wave vector of the incident plane wave describing a 180° sector in a plane (P) containing the axis of the cone-sphere, and for two polarizations: HH [E being in (P)] and VV [E being perpendicular to (P)]. The angle of incidence 0° corresponds to the wave whose vave vector is carried by the axis of the cone and directed from the cone toward the sphere.

The grid for the surface Γ_c is shown in figure 3. It has 1,610 nodes and 3,216 triangular elements.
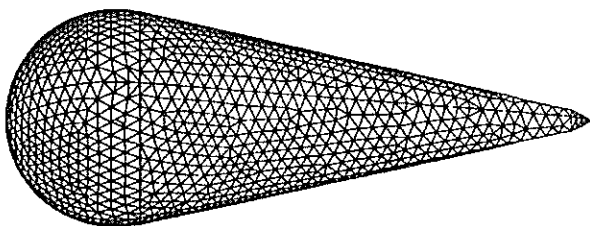
Fig. 3. — Grid for metal cone-sphere.

The results of the computation are shown in figure 4 for the HH polarization and figure 5 for the VV polarization, reading the ordinate in

$$10 \log_{10} \lim_{R \to \infty} \frac{4\pi R^2 \| E_r \|^2}{\pi a^2 \| E_i \|^2}$$
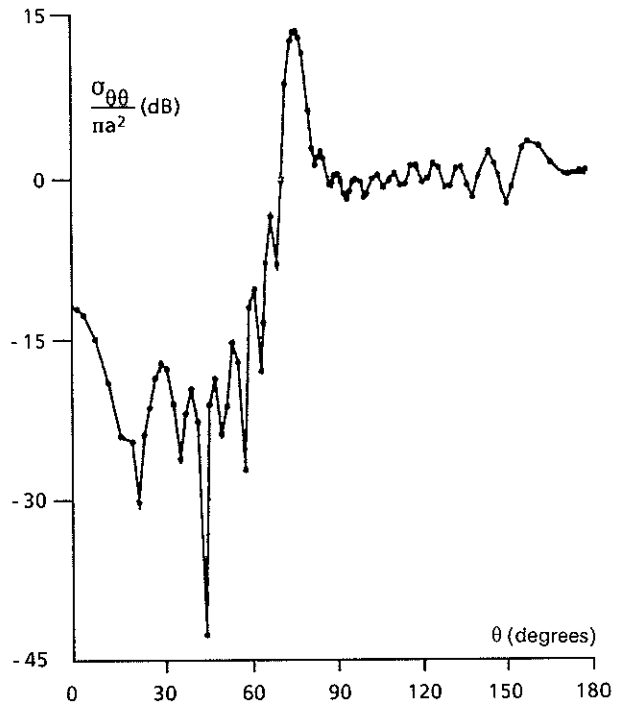
Fig. 4. — HH polarization. RCS of a cone-sphere with 12.5° semi-angle at wavelength $\lambda = 0.974$ a (a being the radius of the spherical part).
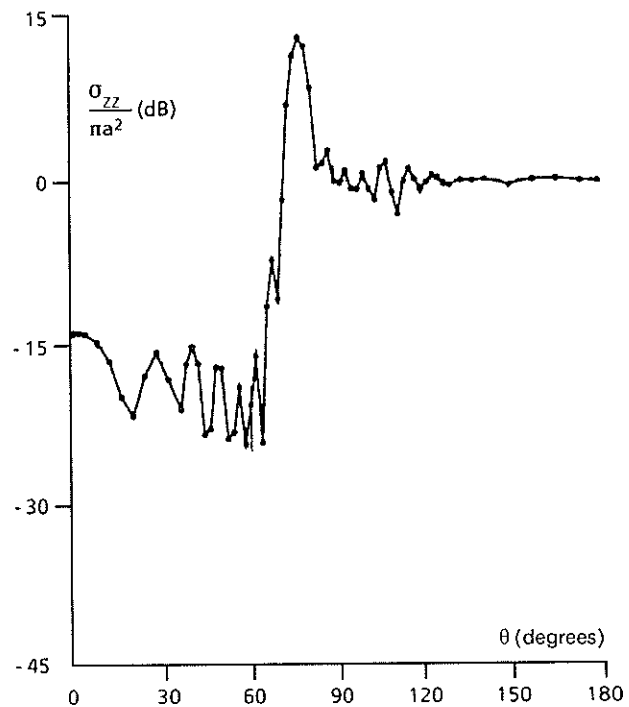
Fig. 5. — VV polarization. RCS of a cone-sphere with 12.5° semi-angle at wavelength $\lambda = 0.974$ a (a being the radius of the spherical part).

V,1.3. — *Metal Dihedron*

The object is a wedge consisting of two perpendicular rectangular metal plates measuring 0.10 m × 0.15 m and 0.001 m thick, assembled along their greater length.

The RCS is studied for the wavelength λ = 0.066 7 m (4.5 GHz) and the wave vector of the incident plane describes a 120° sector in a plane (P) normal to the edge of the dihedron. The incidence origin corresponds to the wave vector in the plane of the dihedral bisector, directed toward the acute angle. Two polarizations are considered: HH [the electric field E is in (P)] and VV polarization [E perpendicular to (P)].

The grid of the surface Γ_c is shown in figure 6. It has 778 nodes and 1,552 triangular elements.
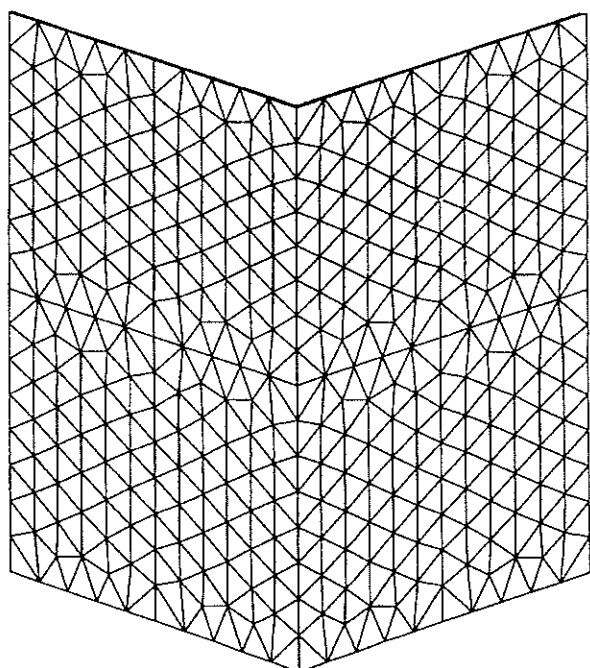
Fig. 6. — Grid for metal dihedron.

The computer results are shown in figure 7 for the HH polarization and figure 8 for the VV, reading the
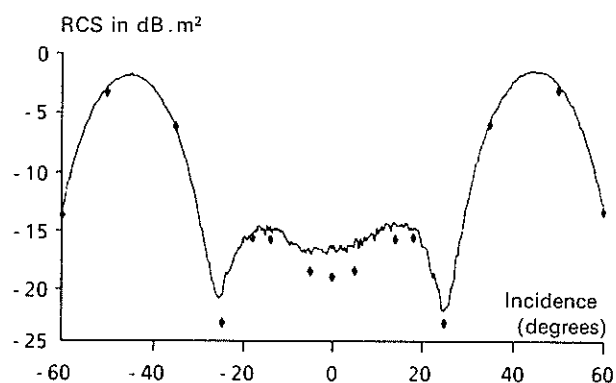
Fig. 7. — HH polarization. RCS of a right dihedron (two plates measuring 10 × 15 × 0.1 cm, set at 90°) at 4.5 GHz.
◆ Numerical
— Measurements (ONERA/DES Camera 1)
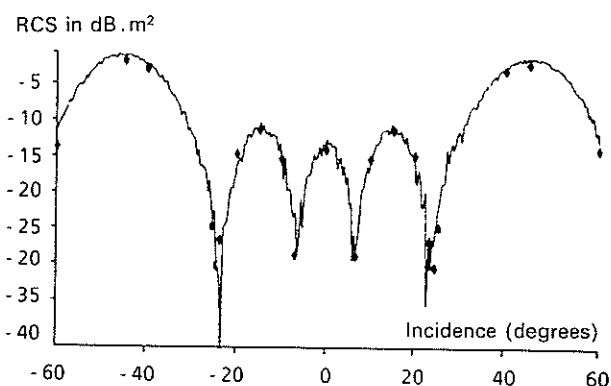
Fig. 8. — VV polarization. RCS of a right dihedron (two plates measuring 10 × 15 × 0.1 cm, set at 90°) at 4.5 GHz.
◆ Numerical
— Measurements (ONERA/DES Camera 1)

ordinate in $10 \log_{10} \lim_{R \to \infty} 4\pi R^2 \dfrac{\|E_r\|^2}{\|E_i\|^2}$.

The good agreement is visible between the numerical predictions and experimental measurements, taken from a study by ONERA's Systems Department.

V,2. — CASE OF A HOMOGENEOUS DIELECTRIC SPHERE

We now consider a nonlossy, homogeneous, isotropic dielectric sphere of radius $a = 1$ m with the following characteristics:

Case 1: Wavelength $\lambda = 1.8$ m, $\varepsilon^* = 1.25 - 0.56 j$ [*see* formula (12) in Part I] and $\mu^* = \mu = 1.1$ [*see* formula (4) in Part I].

Case 2: $\lambda = 2.3$ m, $\varepsilon^* = 1.25 - 0.56 j$ and $\mu^* = \mu = 1.0$.

The bistatic cross section is studied for two planes: HH (plane defined by wave vector k and electric field E_i) and VV (plane defined by k and H_i) for an angular sector of 180°, with the angle origin corresponding to the backscattered cross section.

A partial view of the grid is given in figure 9. The outer surface Γ_d has 441 nodes and 878 triangular elements. The dielectric volume is meshed by 1,304 nodes and 6,346 tetrahedrons.

The computed results are compared with the analytical in figures 10 and 11 for case 1, and figures 12 and 13 for case 2. The ordinates read $10 \log_{10} \lim_{R \to \infty} 4\pi R^2 \dfrac{\|E_r\|^2}{\|E_i\|^2}$. The numerical results can be seen to agree well with the analytical reference solution.

The results for this case validate the surface integral operators and dielectric volume differentials as well as the magnetic induction zero divergence constraint.
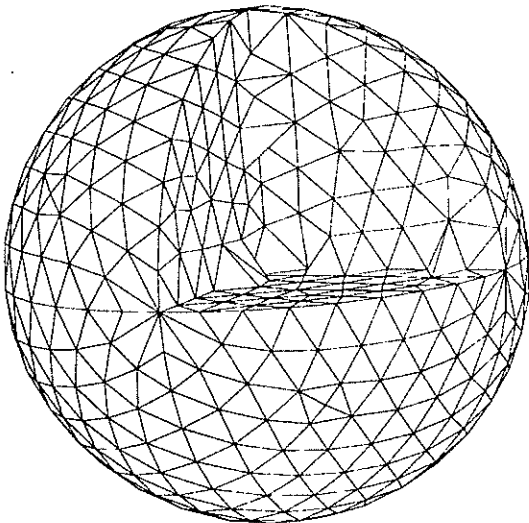
Fig. 9. — Partial and cutaway view of grid
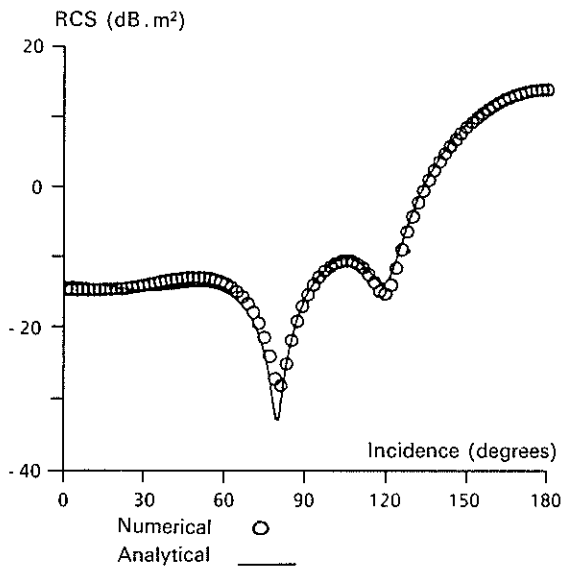for homogeneous dielectric sphere.

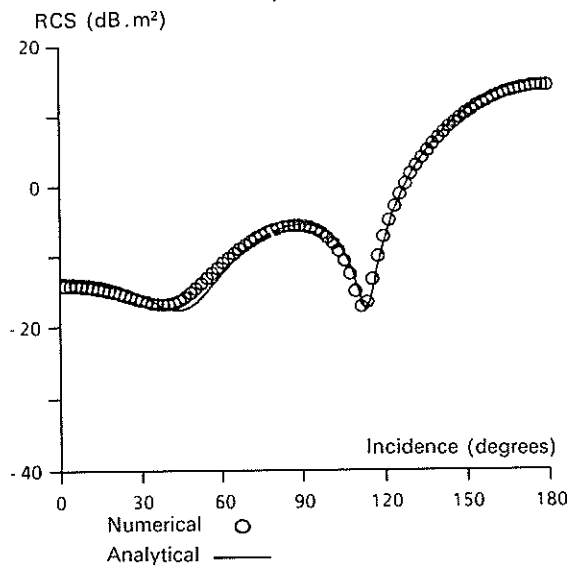

Fig. 10. — HH polarization, λ = 1.8 m.
Dielectric sphere.

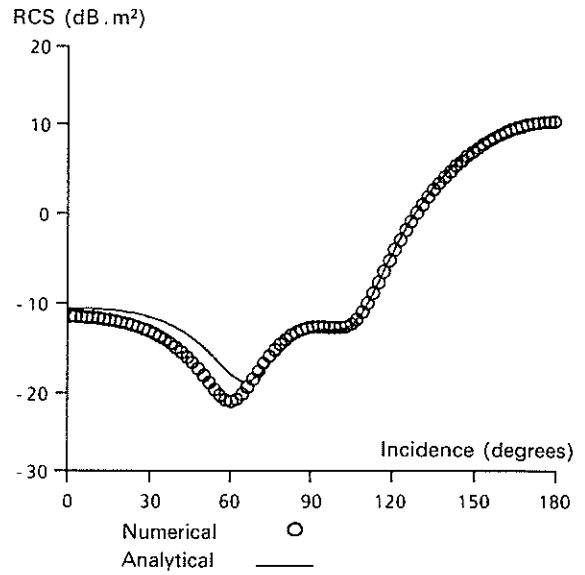

Fig. 11. — VV polarization, λ = 1.8 m.
Dielectric sphere.

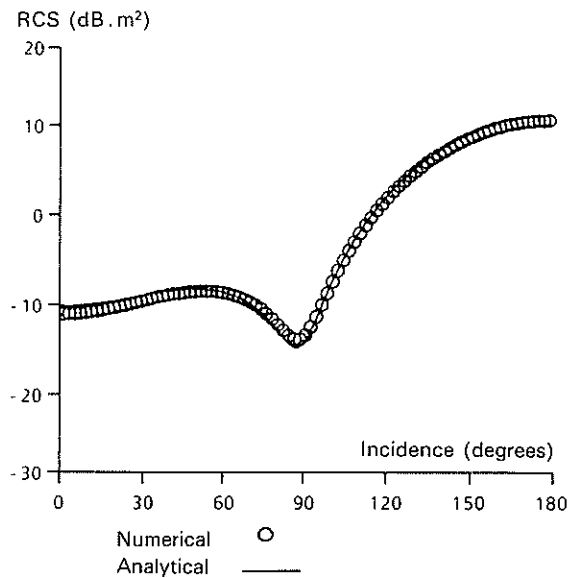
Fig. 12. — HH polarization, λ = 2.3 m.
Dielectric sphere.

Fig. 13. — VV polarization, λ = 2.3 m.
Dielectric sphere.

V,3. — CASE OF A HOMOGENEOUS DIELECTRIC SPHERE WITH METAL CORE

Let us now consider a metal sphere of radius $a_i = 0.8$ m coated with a spherical dielectric layer, 0.2 m thick. The dielectric is homogeneous and isotropic. Two cases are considered.

Case 1: Wavelength $\lambda = 1.8$ m, $\varepsilon^* = 1.25 - 0.56 j$ and $\mu^* = \mu = 1.1$ (there is no magnetic loss in this case).

Case 2: $\lambda = 2.3$ m, $\varepsilon^* = 2.0 - 1.0 j$ and $\mu^* = 1.5 - 1.0 j$ (with magnetic losses).

The bistatic cross section is analyzed as in section V,2.

A partial view of the grid is given in figure 14. The outer surface Γ_d has 356 nodes and 708 three-node elements. The inner surface Γ_{cd} has 289 nodes and 574 three-node elements. The dielectric volume is meshed by 672 nodes and 2,073 tetrahedra.
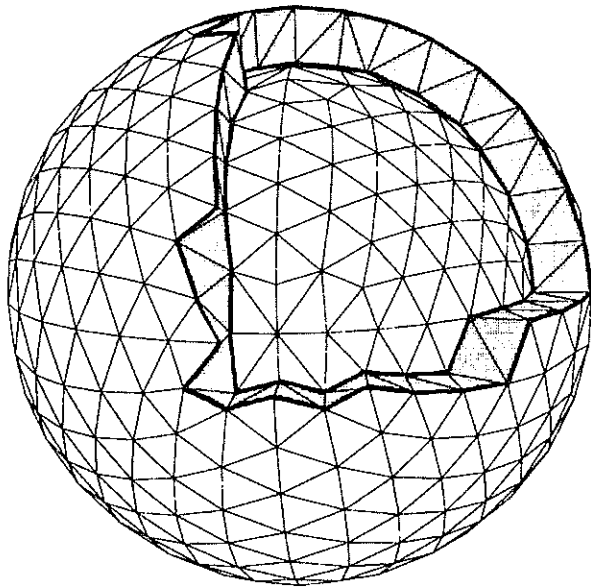
$$10 \log_{10} \lim_{R \to \infty} 4\pi R^2 \frac{\| E_r \|^2}{\| E_i \|^2}.$$ Here again, a good agreement can be seen between the present theory and the analytical reference solution.
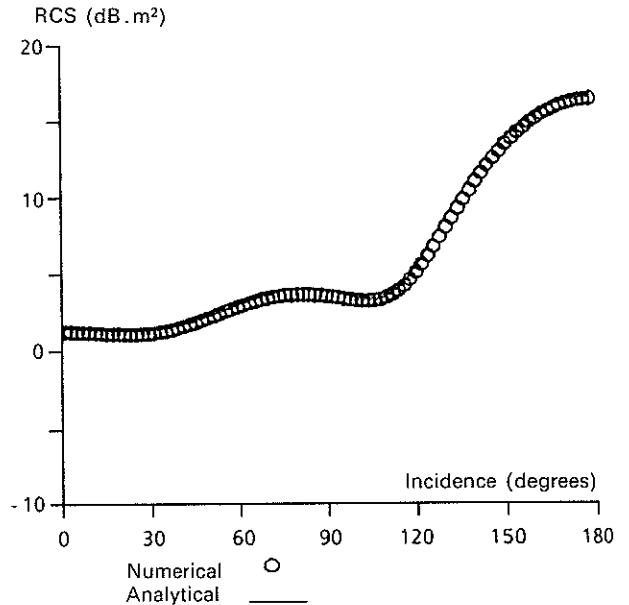

Fig. 14. — Partial and cutaway of grid for dielectric sphere with metal core.

Fig. 16. — VV polarization, $\lambda = 1.8$ m. Dielectric sphere with conductive core.

The computations are compared with analytical results in figures 15 and 16 for case 1 and figures 17 and 18 for case 2, reading the ordinate in
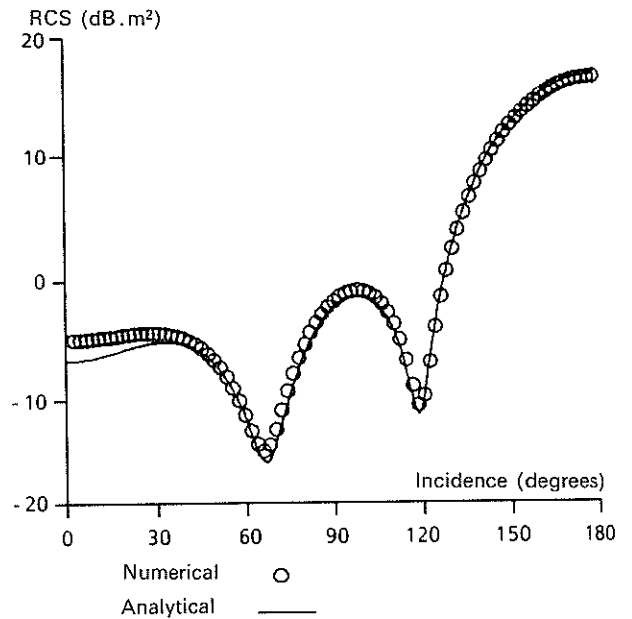

Fig. 17. — HH polarization, $\lambda = 2.3$ m. Dielectric sphere with conductive core.

Among other things, this case validates the treatments of the interfaces of the Γ_{cd} type between a dielectric and a perfect conductor. It has been verified that the presence of the metal core does influence the solution.

Fig. 15. — HH polarization, $\lambda = 1.8$ m. Dielectric sphere with conductive core.

RCS (dB.m²)

Fig. 18. — VV polarization, λ = 2.3 m.
Dielectric sphere with conductive core.
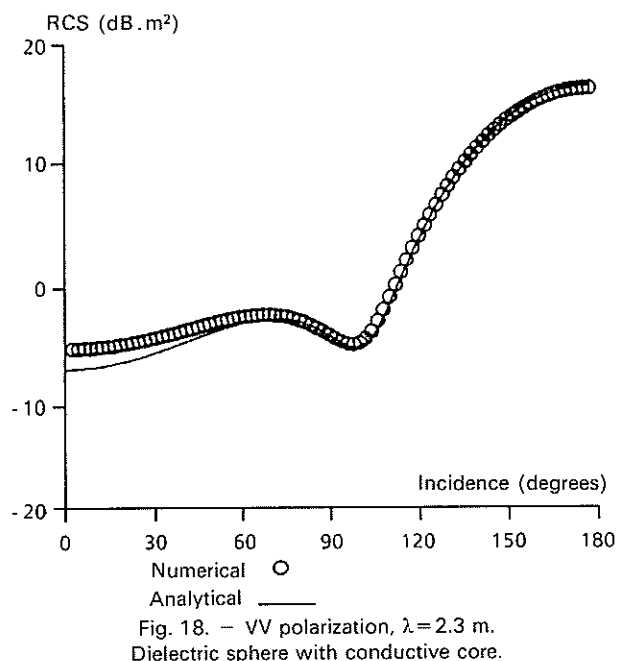
V,4. — INHOMOGENEOUS DIELECTRIC SPHERE

As a last example, we present the case of an inhomogeneous dielectric sphere consisting of one internal dielectric sphere of radius $a_i = 0.7$ m, coated with a dielectric layer 0.3 m thick.

The core sphere is a lossy, isotropic, homogeneous dielectric and its relative characteristics are $\varepsilon^* = 1.25 - 0.56 j$ and $\mu^* = 1.0 - 0.3 j$. The dielectric layer is also homogeneous and isotropic, but its relative characteristics are $\varepsilon^* = 1.21 - 0.15 j$ and $\mu^* = 1.0 - 0.15 j$.

The bistatic cross section is analyzed as in section V,2 for two wavelengths $\lambda = 1.8$ m and $\lambda = 2.3$ m.

Figure 19 gives a partial view of the grid. The outer surface Γ_d has 466 nodes and 888 three-node
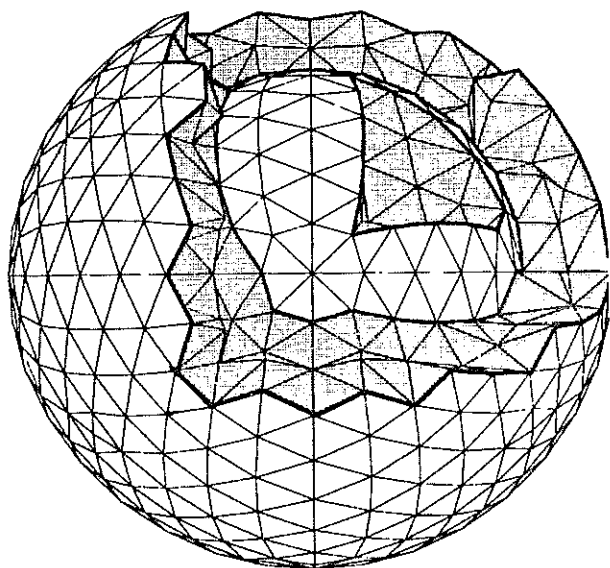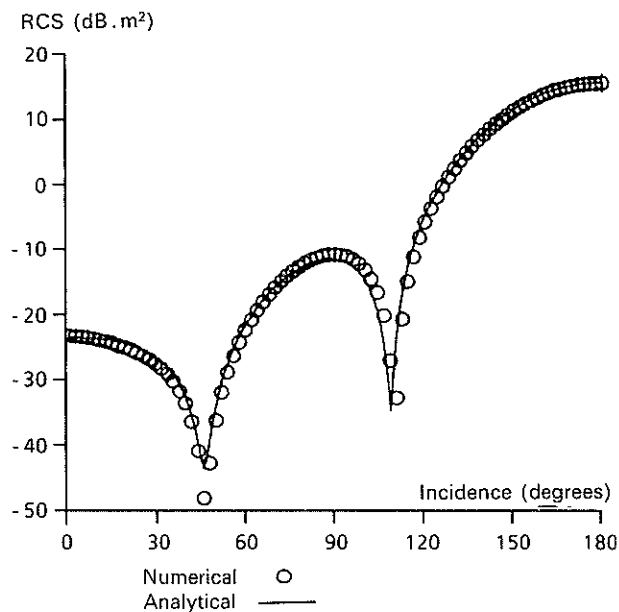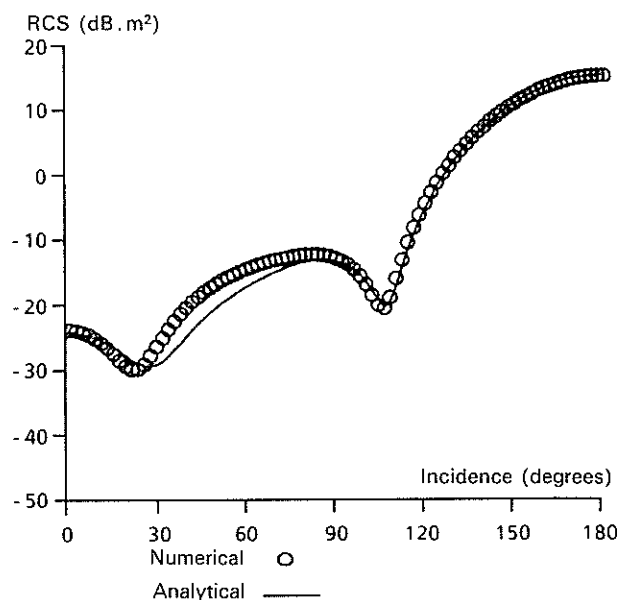

Fig. 19. — Partial and cutaway view of grid for inhomogeneous dielectric sphere.

elements. The inner surface $\Gamma_{nn'}$ has 226 nodes and 448 triangular elements. The total volume of the two dielectrics is meshed with 1,574 nodes and 6,416 tetrahedral elements.

The computed data is compared with the analytical reference in figures 20 and 21 for $\lambda = 1.8$ m

RCS (dB.m²)

Fig. 20. — HH polarization, λ = 1.8 m.
Dielectric sphere in two concentric layers.

RCS (dB.m²)

Fig. 21. — VV polarization, λ = 1.8 m.
Dielectric sphere in two concentric layers.

and figures 22 and 23 for $\lambda = 2.3$ m, reading $10 \log_{10} \lim_{R \to \infty} 4 \pi R^2 \frac{\| E_r \|^2}{\| E_i \|^2}$ on the ordinate. Among other things, this case validates the formulation of the transmission conditions on $\Gamma_{nn'}$ type interfaces between two dielectrics. We have verified that the presence of each dielectric actually does affect the solution.
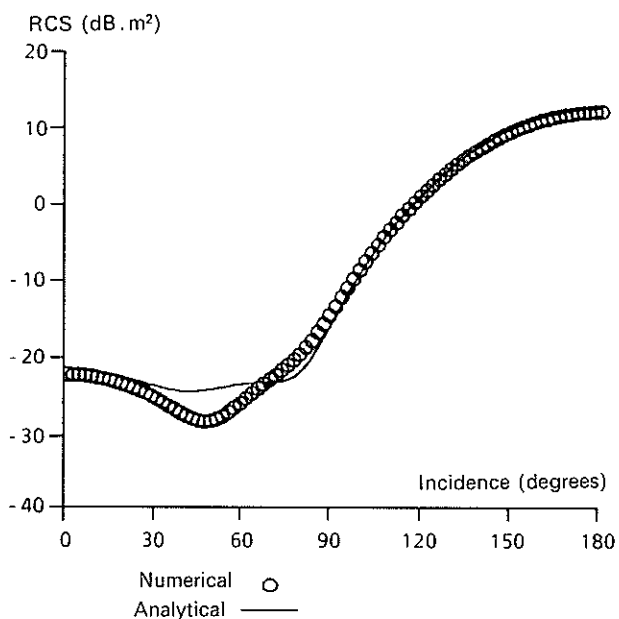
RCS (dB.m²)

Fig. 22. — HH polarization, λ = 2.3 m.
Dielectric sphere in two concentric layers.

RCS (dB.m²)
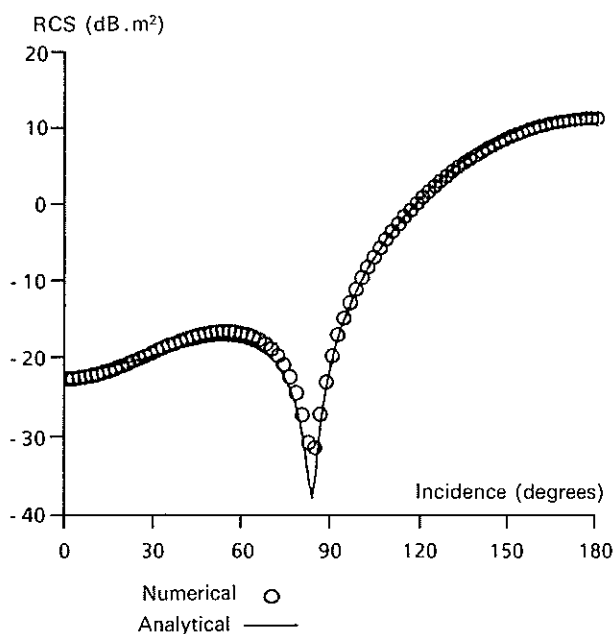

Fig. 23. — VV polarization, λ = 2.3 m.
Dielectric sphere in two concentric layers.

VI. — CONCLUSION

In the framework of linear system solvers based on the use of iterative algorithms, we have presented a strict extension of the Generalized Conjugate Residual method that makes it possible to treat the systems including constraints. This algorithm is adapted to a numerical process in the framework of the solution of Maxwell equations, and the results are as expected.

We have developed a first version of a general 3-D code dubbed HEM 3D. The various applications we have made validate the whole of the theoretical and numerical explanations in Parts I, II and the present Part III of this publication.

This gives us a code for dealing with hybrid multi-conductor-multidielectric volumes for general three-dimensional geometric situations, and with dielectric materials that may be locally inhomogeneous and anisotropic. Wire elements and surface impedances, which would make certain modelings easier, should be introduced in this theory and in the code.

REFERENCES

[1] ANGÉLINI J. J. and SOIZE C. — *Méthode numérique mixte : équation intégrale — éléments finis, pour la SER harmonique 3-D. Partie I : Formulation et analyse numérique.* ONERA (Septembre 1989), Rapport Technique n° 5/2894 RN 081 R.

[2] ANGÉLINI J. J., SOIZE C. and SOUDAIS P. — *Méthode numérique mixte : équation intégrale — éléments finis, pour la SER harmonique 3-D. Partie II : Algorithmes itératifs de résolution.* ONERA (Février 1990), Rapport Technique n° 7/2894 RN 081 R.

[3] AXELSSON O. — *Solution of linear systems of equations : iterative methods.* Sparse matrix techniques, Springer Lecture Notes in Math., 572, V. A. Barker, (1977).

[4] AXELSSON O. — *Conjugate gradient type methods for unsymmetric and inconsistent systems of linear equations.* Linear Algebra Applications, vol. 29, (1980), p. 1-16.

[5] AXELSSON O. — *A generalized Conjugate Gradient, least square methods.* Numerical Mathematics, vol. 51, (1987), p. 209-227.

[6] AXELSSON O. — *A Restarted Version of a Generalized Preconditioned Conjugate Gradient Method.* Applied Numerical Methods, vol. 4, (1988), p. 521-530.

[7] CIARLET P. G. — *Introduction à l'analyse numérique matricielle et optimisation.* Masson, Paris, (1988).

[8] EISENSTAT S. C., ELMAN H. C. and SCHULTZ M. H. — *Variational Iteration Methods for non Symmetric Systems of Linear Equations.* SIAM, J. Num. Anal., vol. 20, (2), (1983), p. 345-357.

[9] HUGHES T. J. R., FERENCZ R. M. and HALLQUIST J. O. — *Large-scale vectorized implicit calculations in solid mechanics on a Cray X-MP/48 utilizing EBE preconditioned conjugate gradients.* Comp. Meth. Appl. Mech. Engrg., vol. 61, (1987), p. 215-248.

[10] JACKSON J. D. — *Classical Electrodynamics.* John Wiley & Sons Inc., New York, 1975.

[11] JACOBS D. A. H. — *Generalization of the conjugate gradient method to solve complex systems of algebraic equations.* CERL Report RD/L/N 70/80, 1980.

[12] JACOBS D. A. H. — *A generalization of the conjugate gradient method to solve complex systems.* IMA J. Num. Anal., vol. 6, (1986), p. 447-452.

[13] JOHNSON G. and NÉDELEC J. C. – *On the coupling of boundary integral and finite element methods.* Math. Comput., vol. 35, (1980), p. 1063-1079.

[14] JOLY P. – *Présentation de synthèse des méthodes de gradients conjugués.* Math. Mod. Num. Anal., vol. 20, (1986), p. 639-665.

[15] JOLY P. – *Mise en œuvre de la méthode des éléments finis. Chapitre II : Résolution des systèmes linéaires,* Ellipses, Paris, (1990), p. 57-122.

[16] KERSHAW D. – *The incomplete Cholesky-conjugate gradient method for the iterative solution of systems of linear equations.* J. comp. Phys., vol. 26, (1978), p. 43-65.

[17] LASCAUX P. and THEODOR R. – *Analyse numérique matricielle appliquée à l'art de l'ingénieur.* Tomes I et II, Masson, Paris, (1988).

[18] OLLIVRY J. P. – *Recherche sur les méthodes itératives de résolution des grands systèmes linéaires.* ONERA (Mai 1989), Rapport Technique n° 45/3064 RY 086 R.

[19] PETIT R. – *Ondes électromagnétiques.* Masson, Paris, (1989).

[20] RAVIART P. A. and THOMAS J. M. – *Introduction à l'analyse numérique des équations aux dérivées partielles.* Masson, Paris, (1983).

[21] RUCK G. T., BARRICK D. E., STUART W. D. and KRICHBAUM C. K. – *Radar Cross Section Handbook.* G. T. Ruck Éd., Plenum Press, New York, 1970.

[22] SAAD Y. and SCHULTZ M. H. – GMRES: *A generalized minimal residual algorithm for solving nonsymmetric linear systems.* Research Report YALEU/DCS/RR-254, Yale University, 1983.

[23] SARKAR T. K., YANG X. and ARVAS E. – *A limited survey of various conjugate gradient methods for solving complex matrix equations arising in electromagnetic wave interactions.* Wave motion vol. 10, (1988), p. 527-546.

[24] SOIZE C. and SOUDAIS P. – *Méthode numérique mixte : équation intégrale – éléments finis, pour la SER harmonique 3-D. Partie III : Développement et validation du code tridimensionnel tout conducteur.* ONERA (Janvier 1990), Rapport Technique n° 6/2894 RN 081 R.

[25] SOUDAIS P. and SOIZE C. – *Méthode numérique mixte: équation intégrale – éléments finis, pour la SER harmonique 3-D. Partie IV : Première phase du développement du code général 3D multi-conducteur, multi-diélectrique.* ONERA (Décembre 1990), Rapport Technique n° 1/3745 RY 006 R.

[26] STRATTON J. A. – *Théorie de l'électromagnétisme.* Dunod, Paris, (1961).

[27] VAN DER VORST H. A. and DEKKER K. – *Conjugate gradient type methods and preconditionnings.* J. Comp. Appl. Math., vol. 24, (1988), p. 73-87.